Vietnam Journal of Earth Sciences, 46(4), 570-594, https://doi.org/10.15625/2615-9783/21418

Vietnam Journal of Earth Sciences
https://vjs.ac.vn/index.php/jse

Assessing aerosol changes over Delhi using satellite and ground measurement data: Insights from a COVID-19 lockdown period

Huong Nguyen-Thuy[1], Thanh Ngo-Duc[2,*], An Dam-Duy[3]

[1]*Nara Women's University, Nara, Japan*
[2]*University of Science and Technology of Hanoi, VAST, Hanoi, Vietnam*
[3]*Center for Calibration of Environmental and Chemical Equipment, Hanoi, Vietnam*

Received 03 June 2024; Received in revised form 08 July 2024; Accepted 28 August 2024

ABSTRACT

The tragic COVID-19 pandemic, while presenting numerous devastating consequences, has inadvertently provided a unique opportunity for studying air pollution. In this study, we specifically evaluate the spatiotemporal changes in aerosols before and during the COVID-19 lockdown from March to May 2020 over Northwest India, with a particular focus on two subregions in the vicinity of Delhi: Delhi-West and Delhi-East. The assessment was conducted using aerosol optical depth (AOD) data from the Moderate Resolution Imaging Spectroradiometer (MODIS) mission, aerosol profiles from the Cloud-Aerosol Lidar and Infrared Pathfinder Satellite Observation (CALIPSO) mission, and ground-based measurements of PM2.5 and PM10. Results demonstrated evident reductions in surface particulate matter and AOD during the lockdown. Approximately 40% of the contribution to the total AOD was from aerosols below 1 km. Different rates of change in AOD were observed for the two subregions across different lockdown phases, attributed to differences in emission sources: Delhi-East is more influenced by residential emissions, while Delhi-West is more affected by natural sources. The surface concentration and variabilities of PM2.5 and PM10 confirmed the differences between the two subregions, emphasizing the role of anthropogenic activities in PM2.5 emissions over the study area.

Keywords: Aerosol, air pollution, CALIPSO, MODIS, Delhi, COVID-19.

1. Introduction

Aerosols play a critical role in the Earth's atmosphere. The amount of aerosols decreases with altitude and has the highest concentration typically found near the surface (Liou, 2002). In the troposphere, aerosol particles can act as nuclei to form clouds and fog and significantly affect chemical reactions occurring in the atmospheric layers (Brasseur et al., 1999; Shiraiwa et al., 2011). The near-surface layer of the atmosphere exhibits a notable concentration of fine aerosols, such as particulate matter that is 2.5 μm or less in diameter (PM2.5), varying spatially, with suburban areas generally experiencing lower levels of PM compared to megacities, particularly in China and India (Lelieveld et al., 2015).

The Delhi National Capital Region (now referred to as Delhi-NCR) in India, which includes Delhi and surrounding districts from the states of Haryana, Uttar Pradesh, and Rajasthan (Fig. 1), is home to over 46 million inhabitants. Within Delhi-NCR, Delhi is known as one of the top polluted cities in the

*Corresponding author, Email: ngo-duc.thanh@usth.edu.vn

world in terms of high PM concentrations. For instance, in early November 2016, PM2.5 levels in Delhi reached 563 μg.m^{-3} (Kanawade et al., 2020), far exceeding the World Health Organisation (WHO) recommended air quality guideline (AQG) levels of 5 μg.m^{-3} for the annual average and 15 μg.m^{-3} for the 24-hour average (WHO, 2021). The sources of PM in the city include vehicular emissions, industrial processes, construction activities, and biomass burning (WHO, 2016). These sources may originate locally due to rapid urbanization and industrialization (Jethva et al., 2018) or be transported from remote areas through atmospheric circulation. The western side of Delhi-NCR experiences the influence of mineral dust transported from Southwest Asia deserts during the pre-monsoon period (Gautam et al., 2009). Pandithurai et al. (2008) provided insights into the aerosol radiative forcing during dust events over the area, indicating that higher aerosol-induced heating in the pre-monsoon period has an impact on the regional monsoon climate. Meanwhile, the eastern side of Delhi-NCR is located near the central part of the Indo-Gangetic Plains (IGP) region, receiving aerosols transported from the highly urbanized areas in the northwestern part of Delhi-NCR by northwesterly wind in pre-monsoon (Liu et al., 2018; Nirwan et al., 2024). Furthermore, the eastern side of Delhi-NCR has a higher population density than the western side (Balk et al., 2019). Note that high population density and vehicular traffic can result in significant emissions of pollutants and aerosol loading in the atmosphere (Guttikunda and Mohan, 2014; Sharma and Joshi, 2016).

The tragic COVID-19 pandemic, which peaked during 2020–2022 while presenting numerous devastating consequences, has inadvertently provided a unique opportunity for studying air pollution. Some prior studies demonstrated that the cessation of many anthropogenic activities in Delhi during some lockdown periods, e.g., from March 22 to May 31, 2020, led to air quality improvements, i.e., a reduction in PM concentrations (e.g., Mahato et al., 2020; Dhaka et al., 2020). However, some other studies reported contrasting findings, with certain phases showing significant improvement in air quality while others observed an increase in aerosol optical depth (AOD) during the lockdown periods (Mahato et al., 2020; Pandey and Vinoj, 2021; Soni, 2021; Venkat-Ratnam et al., 2021; Sharma et al., 2022). It is worth noting that the lockdown periods, from March 22 to May 31, 2020, in these studies above coincided with the pre-monsoon time. On another note, the pre-monsoon time corresponds to a high frequency of air mass updrafts, 77% (Tripathi et al., 2007), up to 4–5 km (Mishra and Shibata, 2012). Hence, the changes in pollutant concentration detected during the COVID-19 lockdown periods might be attributable to local emissions and those originating from higher altitudes of the atmosphere. However, information on aerosol changes in different regional tropospheric layers remains limited.

This study focuses on assessing aerosols' horizontal and vertical changes above Delhi-NCR in India during a COVID-19 lockdown period in 2020. Specifically, we hypothesize that aerosol changes in the two regions, Delhi-West and Delhi-East, might differ based on their sources, whether local or transported from distant regions. To elucidate this hypothesis, we describe the analysis using different observational data sources of aerosols: remote sensing satellite data and in situ station data in the following sections.

The rest of this paper is composed of three sections. Section 2 describes the study area, period, datasets, and analysis methods. In Section 3, we present the results, examining the spatial change of aerosols and vertical distribution of observed optical parameters in the atmosphere above Delhi-NCR, as well as

the changes of PM2.5 in the planetary boundary layer. This section notably focuses on the two distinct subregions, Delhi-West and Delhi-East, with different climatic and urbanized characteristics observed before and during the lockdown period of the COVID-19 pandemic. Finally, conclusions are presented in Section 4.

2. Data and Methodology

2.1. Study area: geographical setting

We conduct the analysis over Northwest India and then focus on the Delhi-NCR area (Fig. 1). Additionally, we examine two distinct subregions characterized by different climatic and urbanized features: the west side (hereinafter referred to as Delhi-West) and the east side of Delhi-NCR (hereinafter referred to as Delhi-East), which encompass the areas of [27.9°N–29.3°N, 75.9°E–77.2°E] and [27.9°N–29.3°N, 77.7°E–79°E], respectively (Fig. 1). It is worth noting that Delhi-West belongs to the humid subtropical climate zone, while Delhi-East is in the arid zone (Dimitrova and Bora, 2020). Therefore, we expect different types of aerosols and different sources to be present in these two suburban regions.

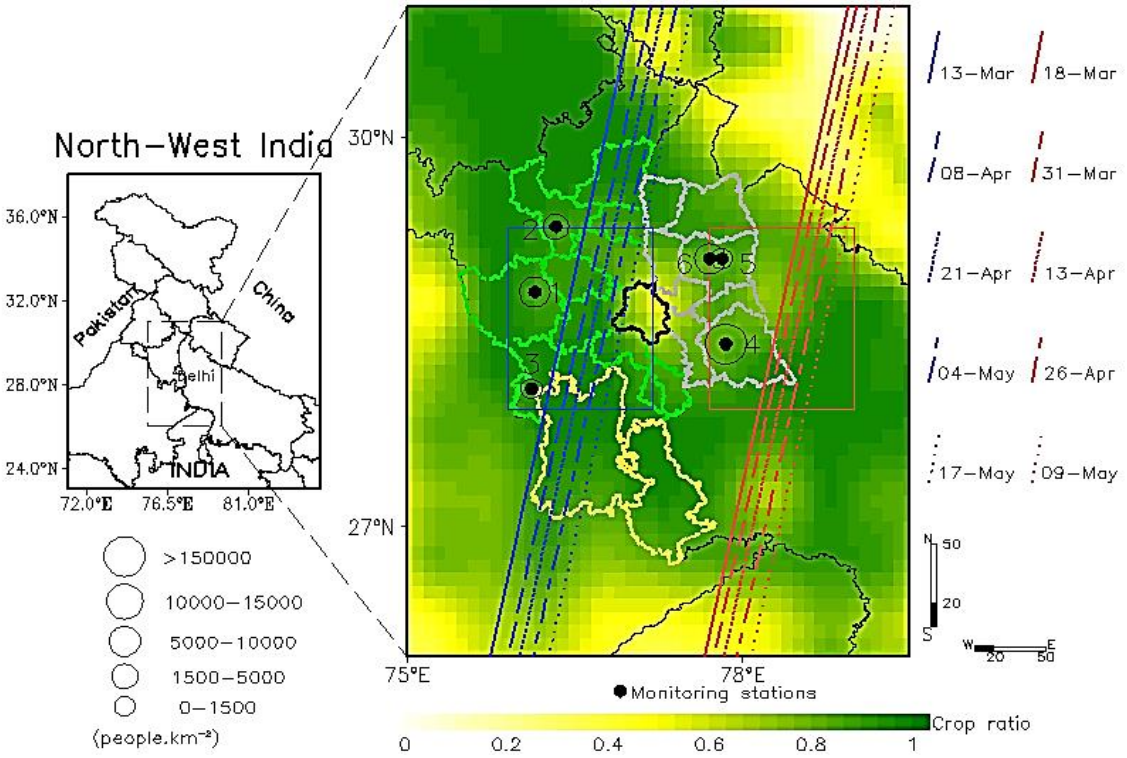

Figure 1. Map of Northwest India (left) with Delhi-NCR (black box) and map of the study area (right), including Delhi (thick black contour), the districts of Haryana state (green contour), Uttar-Pradesh state (gray contour), and Rajasthan state (yellow contour). Two distinct subregions, Delhi-West and Delhi-East, are delineated by the red and blue squares, respectively. The CALIPSO footprints over Delhi-West (blue lines) and Delhi-East (red lines) from March to May 2020, the fraction of cropland area (shaded), the locations of monitoring stations (black dots), along with corresponding population density at those stations (black circles, with the size indicating the density), are also displayed. Data on cropland areas were downloaded from the Harvard Dataverse (Fujimori et al., 2018). The administrative boundaries are plotted using shape files from Esri India Technologies Private Limited (2023)

2.2. Study period

The study period is from March 1 to May 31, 2006–2020. This March to May period coincides with the pre-monsoon season in the region (Tripathi et al., 2007; Mishra and Shibata, 2012; Mehta et al., 2021). Our focus is on 2020, during which COVID-19 spread, leading to multiple lockdown phases from March to May. The March-May period in 2020 includes a Business as Usual Phase (BAU) and four consecutive lockdown phases (Ministry of Home Affairs, 2020; Misra et al., 2021), respectively referred to as LD01-LD04. Below, we provide further details of each phase in 2020:

- Business as Usual (BAU, March 1-March 22): there were no COVID-19 restrictions in place;
- Phase 1 (LD01, March 23 - April 14): all non-essential services and factories are halted;
- Phase 2 (LD02, April 15 - May 3): following the designated date of April 20, agricultural businesses, public work programs, cargo transportation services, and banking institutions resumed operations;
- Phase 3 (LD03, May 4 - May 17): The zoning lockdown area was shaded as "red," denoting some infection, and "green," denoting no restrictions. Red zones were further divided into containment and buffer zones. Construction activities remained restricted in the red zone, while traffic flow was eased in the green and orange zones;
- Phase 4 (LD04, May 18-May 31): except for places where large crowds congregated, such as shopping centers, colleges, schools, and airplanes, all other activities were allowed.

In section 3 (Results), we compared the aerosol data for the lockdown phases in 2020 with corresponding data from different years spanning 2006–2019, highlighting the sources of aerosols over the region.

2.3. Data

2.3.1. Satellite data

This study used Moderate Resolution Imaging Spectroradiometer (MODIS) data to obtain total aerosol loading throughout the entire atmospheric column. In contrast, Cloud-Aerosol Lidar and Infrared Pathfinder Satellite Observation (CALIPSO) data were used to measure aerosols at different altitudes.

The MODIS mission, launched in 1999, provides AOD information, among other variables (Levy et al., 2018). AOD information is obtained using the Dark Target (DT) algorithm, which relies on the contrast between the dark surface (land or ocean) and the aerosols in the atmosphere to estimate AOD at 0.55 μm. The Deep Blue (DB) algorithm complements the DT by providing better AOD over bright surfaces (Sayer et al., 2013). Since the merged DT and DB products generally offer better coverage and quality compared to using DT or DB alone (Levy et al., 2013; Sayer et al., 2014), we employed in this study the merged daily MODIS AOD product, version 6.1 (Platnick et al., 2015). The data have a resolution of 1° × 1° and were downloaded from https://giovanni.gsfc.nasa.gov/.

Regarding CALIPSO, launched in 2006, its Cloud-Aerosol Lidar with Orthogonal Polarization (CALIOP) instrument measures the vertical profile of aerosols and clouds using backscattering and depolarization techniques. The vertical resolutions of the profiles are 30 m and 60 m at 532 nm and 1064 nm, respectively, at altitudes below 8.2 km (Winker et al., 2009).

CALIPSO provides both daytime and nighttime data. The selected CALIPSO variables in our analysis include (1) the Attenuated Total Backscatter (ATB) at 532 nm; (2) the aerosol sub-types; (3) the total backscatter coefficient at 532 nm; (4) the color ratio (CR), defined as the ratio of the backscatter coefficient of particles at the

wavelength 1064 nm to that at 532 nm; and (5) the particulate depolarization ratio (PDR), defined as the ratio of the perpendicular backscatter component to the parallel backscatter component at the wavelength 532 nm.

All the above variables are Level 2 data obtained from the CALIOP Version 4.51 data with a horizontal resolution of 5 km, except for the ATB, which is Level 1 data with a horizontal resolution of 333 m.

In this study, we selected CALIPSO orbits that passed over Delhi-NCR on the most clear-sky days from March to May 2020. Due to high solar background noise during the day (Liu et al., 2008), nighttime data (descending orbit) were considered. We obtained 10 orbits (Fig. 1), with 5 profiles over Delhi-West and 5 profiles over Delhi-East. The overpass time for the orbit tracks was from 20:00 to 21:00 UTC.

2.3.2. Monitoring station data

To obtain information at the surface, this study utilized continuous ground PM2.5 and PM10 measurement data from six monitoring stations within 100 km of the CALIPSO footprints (Table 1, Fig. 1). All six stations are certified by the Indian Ministry of Environment, Forest and Climate Change (MoEFCC).

Table 1. List of stations, their names, and the distances (in km) to the CALIPSO footprints. The symbol "-" indicates distances exceeding 100 km. HSPCB stands for Haryana State Pollution Control Board, and UPPCB stands for Uttar Pradesh Pollution Control Board

Date	**Station 1** H.B. Colony-Bhiwani-HSPCB	**Station 2** Police-Lines-Jind-HSPCB	**Station 3** Shastri-Nagar-Narmaul-HSPCB	**Station 4** Yamunapuram-Bulandshahr-UPPCB	**Station 5** Ganga-Nagar-Meerut-UPPCB	**Station 6** Pallavpuram-Phase2-Meerut-UPPCB
13-Mar	30.1	23.5	14.8	-	-	-
18-Mar	-	-	-	42.8	59.6	69.7
31-Mar	-	-	-	50.3	67.0	77.2
08-Apr	45.3	38.6	30.0	-	-	97.3
13-Apr	-	-	-	59.3	76.0	86.1
21-Apr	55.2	48.6	40.1	-	97.5	48.6
26-Apr	-	-	-	70.0	86.7	96.8
04-May	66.8	60.1	51.7	-	86.0	75.9
09-May	-	-	-	82.3	98.9	-
17-May	79.8	73.1	64.9	90.7	73.1	62.9

Stations 1 to 3 in Delhi-West are operated by the Haryana State Pollution Control Board (HSPCB) and stations 4 to 6 in Delhi-East are operated by the Uttar Pradesh Pollution Control Board (UPPCB). These stations are equipped with instruments to monitor air pollutants at 15-minute intervals. The 15-minute average value of each parameter is reported to the Central Pollution Control Board (CPCB), which subsequently shares data from these stations at intervals of 15 minutes, 30 minutes, 45 minutes, and 1 hour. These stations are maintained following strict procedures, including daily checks (power supply, data transmission), weekly, monthly, and annual inspections, and instrument zero-point calibration.

The station data and related information in this study were obtained from the CPCB website (https://cpcb.nic.in/). The CPCB ensures data quality through adherence to rigorous protocols for sampling, analysis, and calibration (Dhaka et al., 2020).

2.4. Methodology for assessing aerosol changes

We first examined the horizontal distributions of total aerosol loading, i.e., MODIS-AOD, over the study region during the different lockdown phases to assess variations in aerosol levels and their potential sources. The trend of MODIS-AOD for each year in each study phase during 2006–2019 was assessed using the nonparametric Mann-Kendall test (Kendall, 1938; Mann, 1945) with a statistically significant level of 0.05. The Mann-Kendall test, which has the advantage of not assuming any specific distribution for the data and being robust against outliers and missing values, is widely used for assessing long-term trends in various environmental and climatic variables (e.g. Hamed et al., 2008; Vu-Thanh et al., 2014; Salerno et al., 2023; Kliengchuay et al., 2024), including AOD (Habib et al., 2019).

Subsequently, we calculated the difference in AOD for each year compared to 2020 for the five selected study phases using the Wilcoxon Rank-Sum test (Wilcoxon, 1945). This nonparametric statistical test compares two independent datasets to determine if one tends to have higher or lower values than the other. It ranks all values from both datasets together and then compares the sum of the ranks between them. Like the Mann-Kendall test, the Wilcoxon test assumes no specific data distribution.

Next, we examined aerosol characteristics' vertical distribution using CALIPSO and ground measurement data. Among the CALIPSO variables, the ATB is used to differentiate between different cloud conditions, such as overcast and partly cloudy, and to provide quick information about the aerosol layer extending upwards from the ground (Liu et al., 2009; Hayes et al., 2010). The seven aerosol sub-types provided by the CALIOP profiles give insights into aerosol sources, including clean marine, dust, polluted continental/smoke, clean continental, polluted dust, elevated smoke, and dusty marine (Kim et al., 2018). The total backscatter coefficient indicates aerosol concentration in the atmosphere, while CR values depict particle size. CR values for smoke and polluted urban aerosols are generally less than 0.4, much smaller compared to fresh dust (>0.7) (Wandinger et al., 2011). Small CR values indicate fine particles, whereas large CR values indicate coarse particles. Finally, PDR values reveal additional information on particle sources and shapes. PDR values for fresh and aged dust are generally greater than 0.15, those for aged biomass-burning smoke are less than 0.1, and those for urban aerosols (polluted and fresh) are less than 0.05 (Wandinger et al., 2011). Small PDR values suggest the spherical shape of particles.

Notably, the aerosol information below ~300 m is often missing in CALIPSO data. Therefore, additional surface aerosol information is obtained from monitoring stations. We computed PM2.5/PM10 ratios using data from six monitoring stations within 100km of the CALIPSO footprints. A high PM2.5/PM10 ratio typically indicates the prevalence of fine particles primarily emitted from anthropogenic sources. In contrast, a low PM2.5/PM10 ratio suggests the dominance of coarse particles, often from natural sources such as road dust suspension and natural dust storms (Eeftens et al., 2012; Khodeir et al., 2012; Sugimoto et al., 2016; Fan et al., 2021; Bamola et al., 2024).

In brief, combining the three data sources allows us to obtain a comprehensive view of aerosol changes in both horizontal and vertical directions over the study region. Each data source complements the others: MODIS data provide information on total aerosols in the atmospheric column, CALIPSO exhibits aerosol characteristics across various vertical layers generally above 300 m, and monitoring

stations complete the information of surface-level aerosols.

3. Results and Discussions

3.1. Spatial distribution of AOD values in Northwest India

Figure 2 presents the long-term annual AOD average over Northwest India. AOD values around 20°N along the IGP are higher than those in the surrounding areas, ranging from 0.6 to 1, consistent with findings in other studies (Babu et al., 2013; David et al., 2018). Over the highland areas of India where snow exists, AOD retrievals break down, as indicated in white, showing results similar to previous studies (Gouda et al., 2022; Rani and Kumar al., 2022). The AOD trend during 2006–2019 generally indicates insignificant changes over the region, with notable exceptions over the IGP, where a significant decreasing trend was noted. This decline can be primarily attributed to dust transport and the wet removal of aerosols by monsoon rain (Babu et al., 2013). Additionally, small areas in the bottom right of Fig. 2b, which belong to the central part of India, exhibit significant increasing trends, in line with the findings of Tariq (2022).

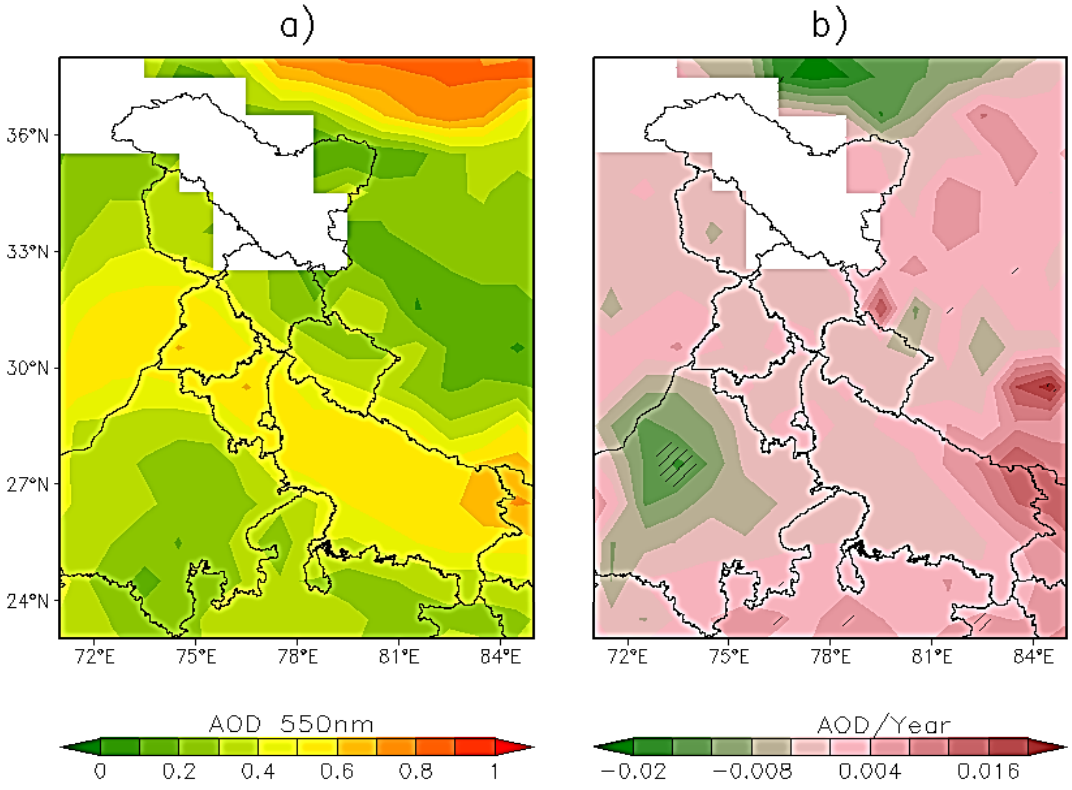

Figure 2. a) Annual average of AOD observed by MODIS and b) trend, spanning 2006–2019 across Northwest India. Hatched patterns indicate regions with statistically significant trends at the 0.05 significance level, while white areas denote missing data

Figure 3 displays the average AOD values of 2020 and 2006–2019 across the different study phases. Similar to the long-term annual AOD average shown in Fig. 2, AOD values along the IGP for each phase are relatively high compared to those in the surrounding areas in Fig. 3b. During 2006–2019, AOD in Phase 3 and Phase 4 tended to be higher than

in BAU, Phase 1, and Phase 2, possibly due to increased dust storm activity. In 2020, the AOD in the BAU phase was the highest compared to the other phases.

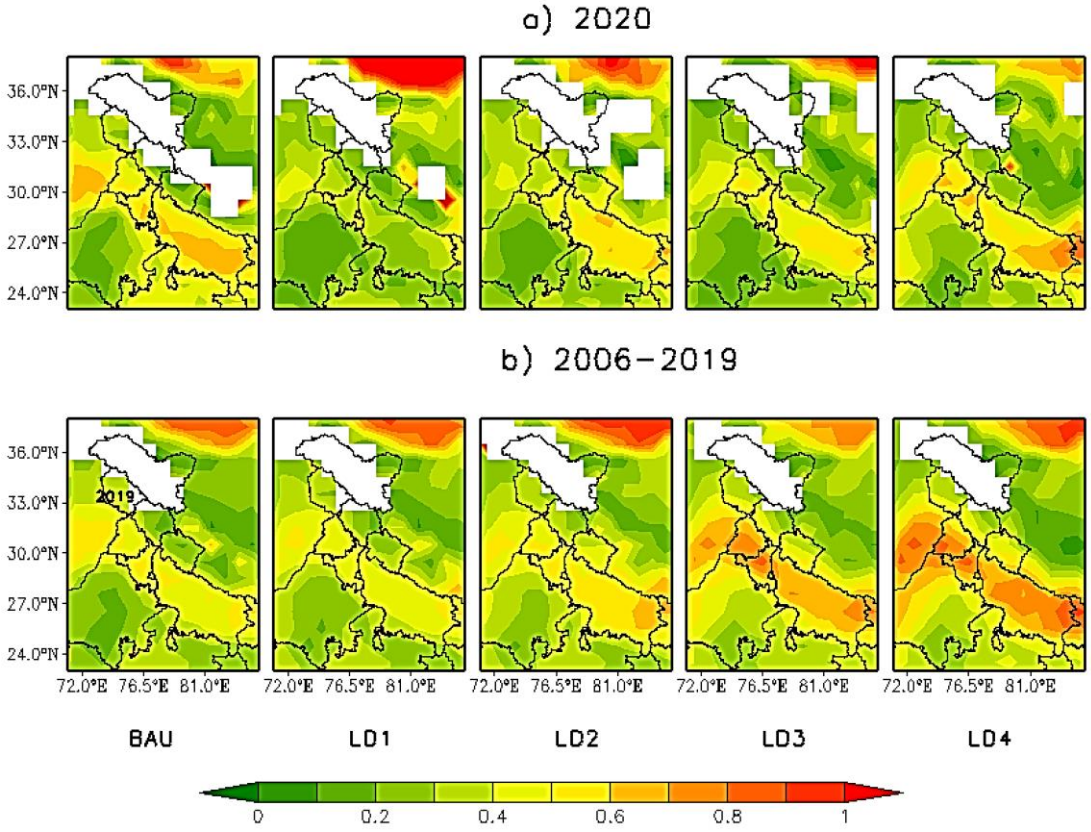

Figure 3. Distribution of AOD observed by MODIS over the different study phases: a) in 2020 and b) the average for the period 2006–2020. White areas denote missing data

Figure 4 further illustrates the differences in AOD between BAU and LD01–LD04 for the year 2020, and that for the period of 2006–2020. Notably, 2020 stands out as a particular year wherein a large area within the study domain, including the IGP and the southern part of Northwest India, experienced a significant decrease in AOD during the lockdown phases compared to BAU, with differences ranging from -0.2 to -0.5. Our findings are consistent with the previous study's results (Pandey and Vinoj, 2021; Soni, 2021; Venkat-Ratnam et al., 2021).

For a closer and more detailed analysis of the sources and variability of aerosols over the region, Fig. 5 zooms into the Delhi-NCR region to examine the distribution of AOD over the different study phases in 2020. Before the lockdown, i.e., during BAU, MODIS observations revealed high aerosol loading over the northwest, southeast, and central areas of Delhi-NCR compared to surrounding areas. Subsequently, during Phase 1, AOD decreased sharply compared to BAU but increased during Phase 2, especially downstream of Delhi in the southeastern part

of Delhi-NCR. Aerosol loading was slightly higher in later phases than in the BAU phase. Notably, the maximum level of AOD in Phase 4 was found in the northwestern part of Delhi-NCR, attributed to the influence of dust storms during this period (Prijith et al., 2021).

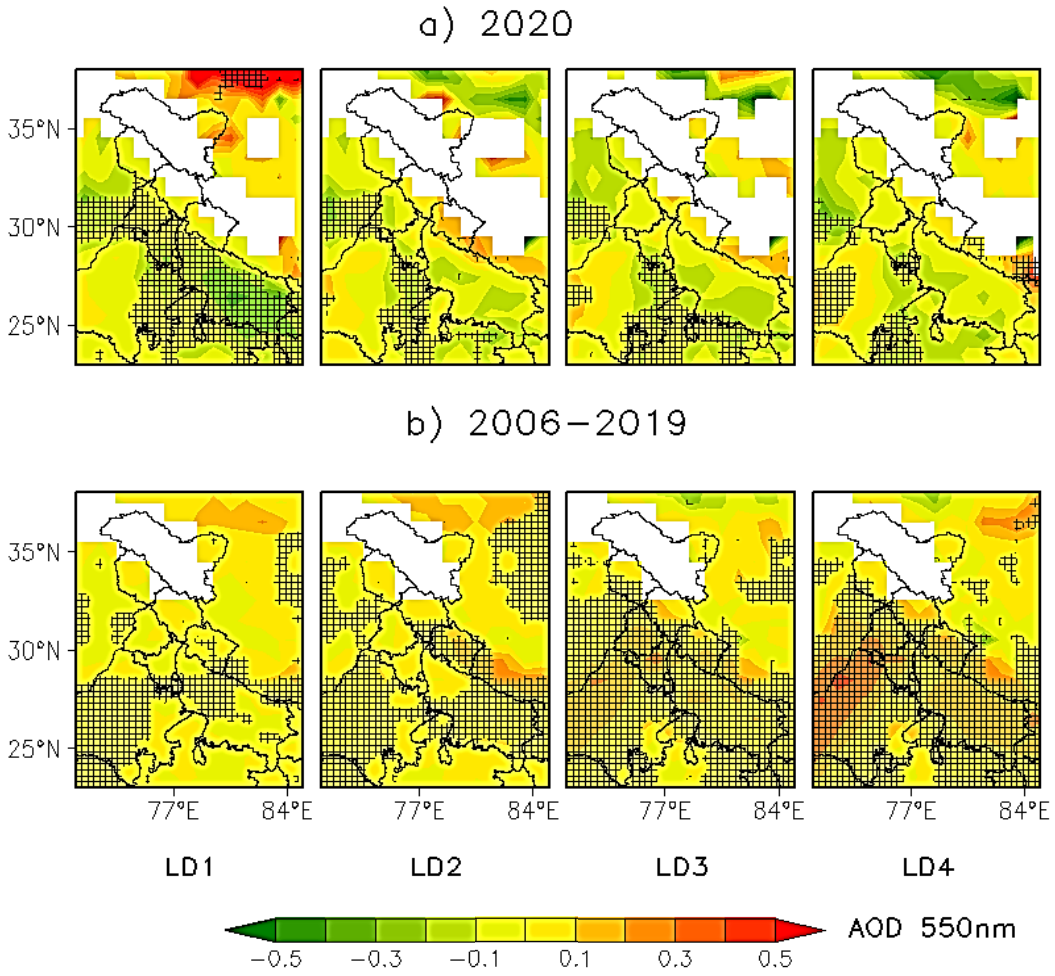

Figure 4. Difference between AOD during Phase 1 to 4 and that during BAU for 2020 and the average for 2006–2020 (shading). Hatched patterns indicate statistically significant differences at the 0.05 level using the Wilcoxon test. White areas denote missing data

In the central area of Delhi-NCR, which includes two regions marked by solid rectangles, Delhi-West and Delhi-East (Fig. 5), during the BAU phase, AOD ranged from 0.5 to 0.6 in the western region (Delhi-West) and 0.45 to 0.5 in the eastern region (Delhi-East). In Phase 1, AOD ranged from 0.3 to 0.4 (Delhi-West) and 0.2 to 0.3 (Delhi-East). Compared to BAU, AOD decreased by approximately 50% in Delhi-West and 44–50% in Delhi-East. In Phase 2, AOD ranged from 0.5 to 0.6 (Delhi-West) and 0.6 to 0.7 (Delhi-East). Compared to BAU, AOD decreased by 25–50% in Delhi-West and 10–20% in Delhi-East. This result implies the effect of aerosols from residential consumption, given the higher population of the Eastern part compared to the Western part of Delhi-NCR, leading to a less

effective reduction in AOD due to local emission activities, such as increased cooking when people stayed home (Sharma and Joshi, 2016). In Phase 3, AOD ranged from 0.35 to 0.4 (Delhi-West) and 0.55 to 0.6 (Delhi-East). In this phase, the decreasing trend of the two regions continued, resulting in a decrease in AOD by 45–55% in Delhi-West and 13–20% in Delhi-East. In Phase 4, AOD ranged from 0.3 to 0.4 in Delhi-West and 0.5 to 0.6 in Delhi-East, indicating decreases of 20–45% and 6–20% in these regions, respectively.

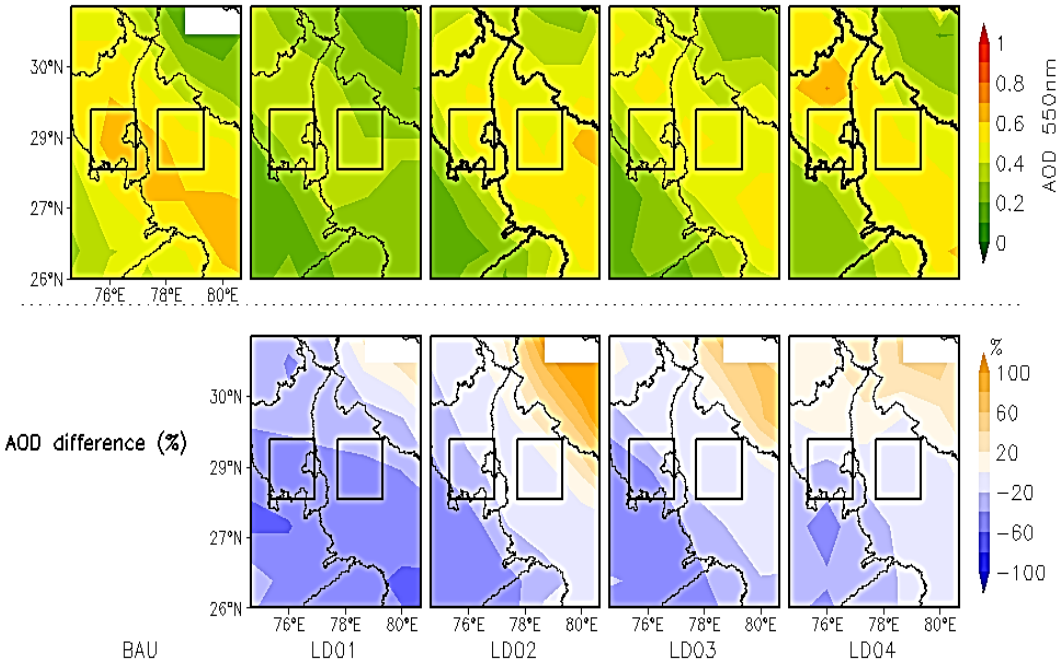

Figure 5. AOD average for the study phases 2020 (above) and the percentage differences between Phases 1 to 4 and BAU (below) over Delhi-NCR

3.2. Vertical changes in aerosols

Figure 6 displays the AOD values provided by MODIS and CALIOP and the average surface PM concentrations provided by monitoring stations during the different lockdown phases in 2020 for the two regions, Delhi-West and Delhi-East. The AOD values were derived from the afternoon measurements by MODIS and nighttime measurements by CALIOP. It is worth noting that CALIOP provides limited data, with a repetitive cycle of about 15-16 days, due to its narrow footprints. However, it has the advantage of a high horizontal resolution, around 333 m.

There are significant differences between the AOD products provided by MODIS and CALIOP. For instance, AOD from CALIOP was significantly higher than AOD from MODIS on March 13 and May 17 in Delhi-West and May 9 in Delhi-East. Additionally, CALIOP provides a broader range of AOD values compared to MODIS, potentially due in part to the higher horizontal resolution of CALIOP. AOD from both subregions tended to decrease in Phase 1 and slightly increase in Phase 2 when less strict lockdown measures were applied. Interestingly, the surface PM concentrations, particularly those of PM10, display similar fluctuations to the AOD variations in Delhi-West. However, these

similar patterns are not always observed in Delhi-East, such as during Phase 4, where there is a noticeable discrepancy between the surface data and MODIS observations. This suggests that the contributions to the AOD values of the total atmospheric column are not solely from surface emissions but also from distant sources and other vertical layers.

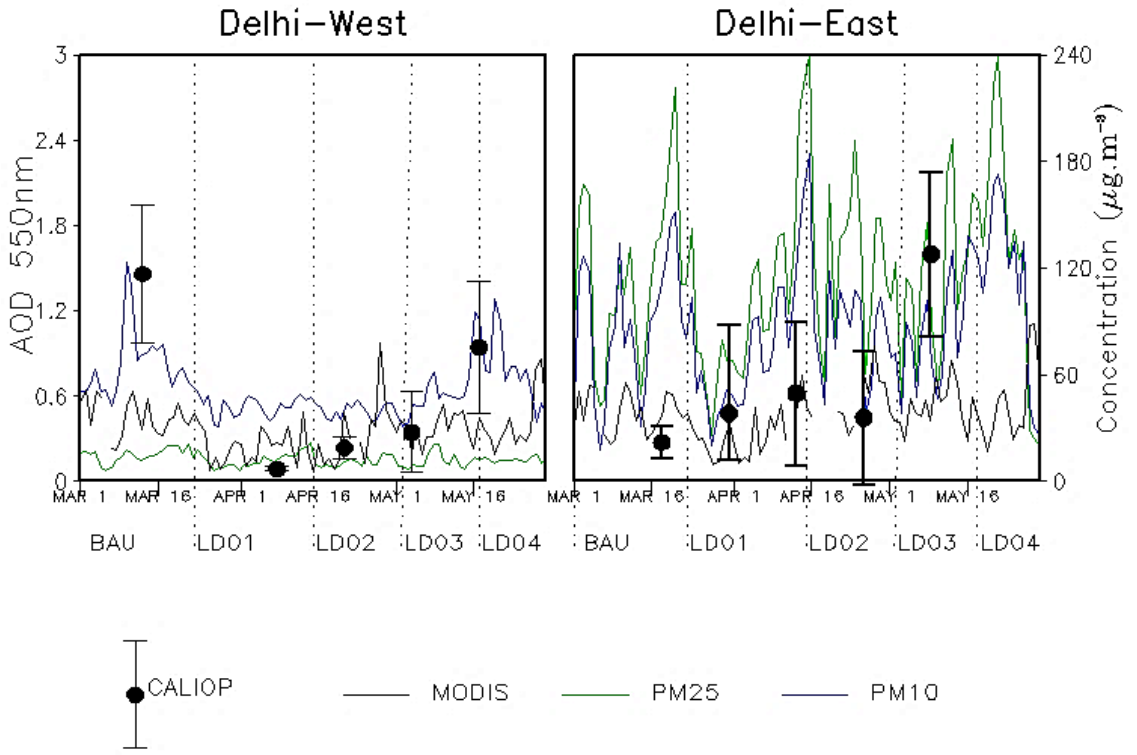

Figure 6. Variation of AOD values during the different lockdown phases in 2020 provided by MODIS and CALIOP and average surface PM concentration provided by monitoring stations for Delhi-West (left) and Delhi-East (right)

It is noted that pollutants' characteristics vary across different vertical layers. For instance, pollutants may have longer mixing time at higher altitudes than at lower altitudes, whereas the most robust mixing rates occur within the boundary layer, usually less than 1 km (Chandra et al., 2014; Sathyanadh et al., 2017; Jethva et al., 2018; Nakoudi et al., 2019). In the upper part of the atmosphere, i.e., the free troposphere, pollutants have a longer lifetime, ranging from several days to weeks. Therefore, it is interesting to compute the AOD in different layers to quantify each layer's contribution to the total AOD.

We separate the vertical CALIPSO profiles into 5 bins: below 1 km, 1–2 km, 2–3 km, 3–4 km, and 4–6 km, as referenced in the study by Mishra and Shibata (2012). Figure 7 presents the percentage of aerosols in each bin that contribute to the total AOD. During the lockdown phases, more than 60% of the contribution to the total AOD was from aerosols above 1 km. On some days, such as April 13, April 21, April 26, May 4, and May 9, the proportion of AOD contribution in the upper layer accounted for more than 70% of the total.

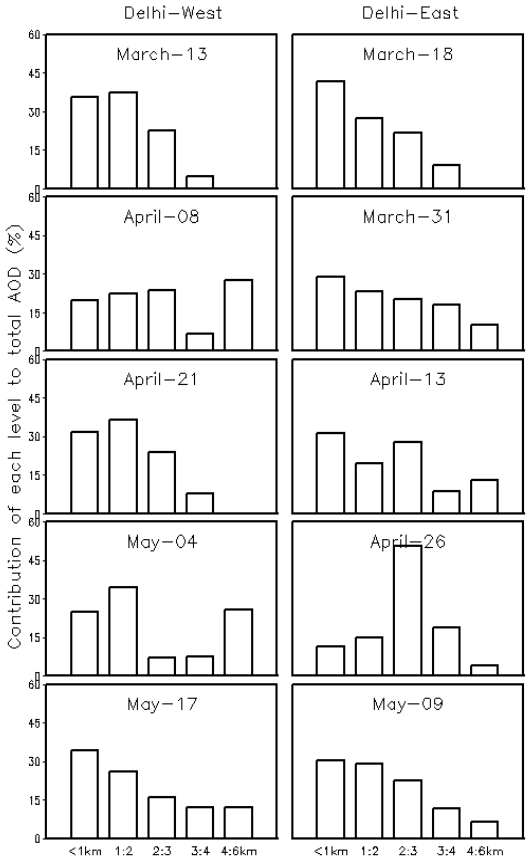

Figure 7. Percentage contribution of AOD from different atmospheric layers to the total columnar AOD. Unit: %

Figure 8 further details the vertical aerosol profiles over Delhi-West by illustrating corresponding observations from MODIS (Aqua + Terra), CALIOP, and the monitoring stations on March 13 (i.e., before the lockdown) and on April 8, April 21, May 4, and May 17 (i.e., during the lockdown).

On March 13, the AOD provided by MODIS was relatively high, at about 0.5-0.8, compared to other dates. The CALIPSO profiles indicate a thick aerosol layer up to 4 km, as observed from the ATB Level 1 signal (2nd row in Fig. 8) and the total backscatter coefficient (4th row in Fig. 8). The total backscatter coefficient was more extensive at lower altitudes, indicating significant aerosol loading. Most aerosols were identified as dust (3rd row in Fig. 8). High CR (> 0.9) and PDR (> 0.25) (5th and 6th rows in Fig. 8, respectively) were found in most of the layers, consistent with the patterns of aerosols described by Mishra and Shibata (2012). This suggests the presence of coarse mode and non-spherical particles (e.g., dust) in the ambient air of the IGP region. These particles can be locally originated or transported from desert areas such as Pakistan and Afghanistan (Dey et al., 2004; Singh et al., 2005; Kumar et al., 2018).

Additionally, Fig. 8 (7th row) shows the ratio of PM2.5/PM10, which provides information about the origin of particulate matter at the three monitoring stations in Delhi-West. Among the monitoring stations, Station 2 (at a higher latitude) shows a relatively high PM2.5/PM10 ratio of 0.52, indicating a dominance of fine-sized particles with an important contribution from anthropogenic emissions. In contrast, Stations 1 and 3 (at lower latitudes) have relatively low PM2.5/PM10 ratios of 0.24 and 0.2, suggesting that these particles might be primarily transported from nearby desert areas such as the Thar Desert in India or Pakistan.

During the lockdown on April 8, the AOD provided by MODIS was 0.1–0.2. The CALIPSO profiles indicate a relatively low ATB intensity. There are two main aerosol layers over the region: the upper layer consists of dust aerosols. In contrast, the bottom layer includes dust and polluted dust (polluted dust is found over the northern part of the region at an altitude of 1–2 km). The total backscatter coefficient (4th row in Fig. 8) recorded shallow values at different altitudes, much lower than March 13, before the lockdown. In the two aerosol layers, the CR (typically > 0.7) and PDR (typically > 0.25) values indicate the dominance of coarse mode and non-spherical particles.

The PM2.5/PM10 ratios observed at the stations in Delhi-West on April 8 display a

similar pattern to those on March 13: relatively low ratios of 0.34 at Station 1 and 0.43 at Station 3 and a high ratio of 0.63 at Station 2. Notably, this day is considered one of the pristine days at the surface level during the lockdown (Dhaka et al., 2020), with the main contribution to aerosols coming from natural sources and almost no contribution from primary anthropogenic sources such as transportation and industry.

On April 21 (Phase 2), the AOD provided by MODIS was 0.4–0.6. The CALIPSO profiles also exhibit a low intensity of attenuated backscatter compared to the pre-lockdown period (March 13) but higher than on April 8 (Phase 1). There is still an apparent reduction of over 80% in aerosol concentrations at different altitudes, as observed from the vertical profile of the total backscatter coefficient (4th row in Fig. 8) compared to March 13, before the lockdown. The aerosol types are mainly polluted dust and dust. The CR is higher than 0.8, indicating coarse-size particles (5th row in Fig. 8). The PDR across different altitudes ranges from 0.1 to 0.45, with most values around 0.15, indicating more spherical particles. These values are lower than those recorded on March 13 and April 8. This reduction in PDR can be explained by external mixing with spherical aerosols, leading to a dilution of dust concentration, or internal mixing (coating) (Sugimoto et al., 2002; Dey et al., 2008). At the surface level, the PM2.5/PM10 ratios are low across the three stations, ranging from 0.3 to 0.5, indicating a minor contribution to aerosols from anthropogenic sources.

On the first day of Phase 3, i.e., May 4, when more construction and traffic activities were allowed, the AOD values ranged from 0.1 to 0.4. The CALIPSO profiles show strong convection forming clouds up to a height of 5 km. On this day, there is a clear presence of smoke and elevated smoke with polluted dust and dust (3rd row in Fig. 8). The presence of elevated smoke combined with dust at high altitudes during this period provides insights into the 'elevated heat pump' hypothesis concerning the aerosol-monsoon link for the Asian summer monsoon (Lau and Kim, 2006; Lau et al., 2006; Nigam and Bollasina, 2010). Specifically, dust and black carbon have been identified as the primary absorbing components of aerosols over the IGP (Lau and Kim, 2006; Gautam et al., 2010). These components heat the air, causing it to rise to high altitudes, thereby influencing the Asian summer monsoon by enhancing moist low-level inflow from the northern Indian Ocean (Lau and Kim, 2006; Lau et al., 2006). The dust and smoke mixture generally results in a low intensity of the vertical backscatter coefficient, a high CR, and a wide range of PDR. The PM2.5/PM10 ratios from Station 1 (belonging to the orange zone), being 0.27, and Station 2 (belonging to the red zone), being 0.08, indicate small contributions of anthropogenic emission. Meanwhile, Station 3 (belonging to the green zone) exhibits a fairly high PM2.5/PM10 ratio, 0.52, indicating more anthropogenic emissions where construction and traffic activities are relaxed.

On May 17, the final day of Phase 3, the AOD obtained from MODIS ranged from 0.3 to 0.8. The CALIPSO profiles revealed strong aerosol convection, including dust and polluted dust, reaching altitudes exceeding 4 km (2nd and 3rd rows in Fig. 8). While the vertical structure of the total backscatter coefficient (4th row) resembled that of March 13, more significant CR and smaller PDR values were observed at altitudes higher than 1 km on May 17 compared to March 13. At altitudes less than 1 km, smaller CR and PDR values were observed, indicating a mix of fine and spherical particles. Data from surface stations indicate PM2.5/PM10 ratios ranging from 0.2 to 0.37, suggesting a minor impact from human activities.

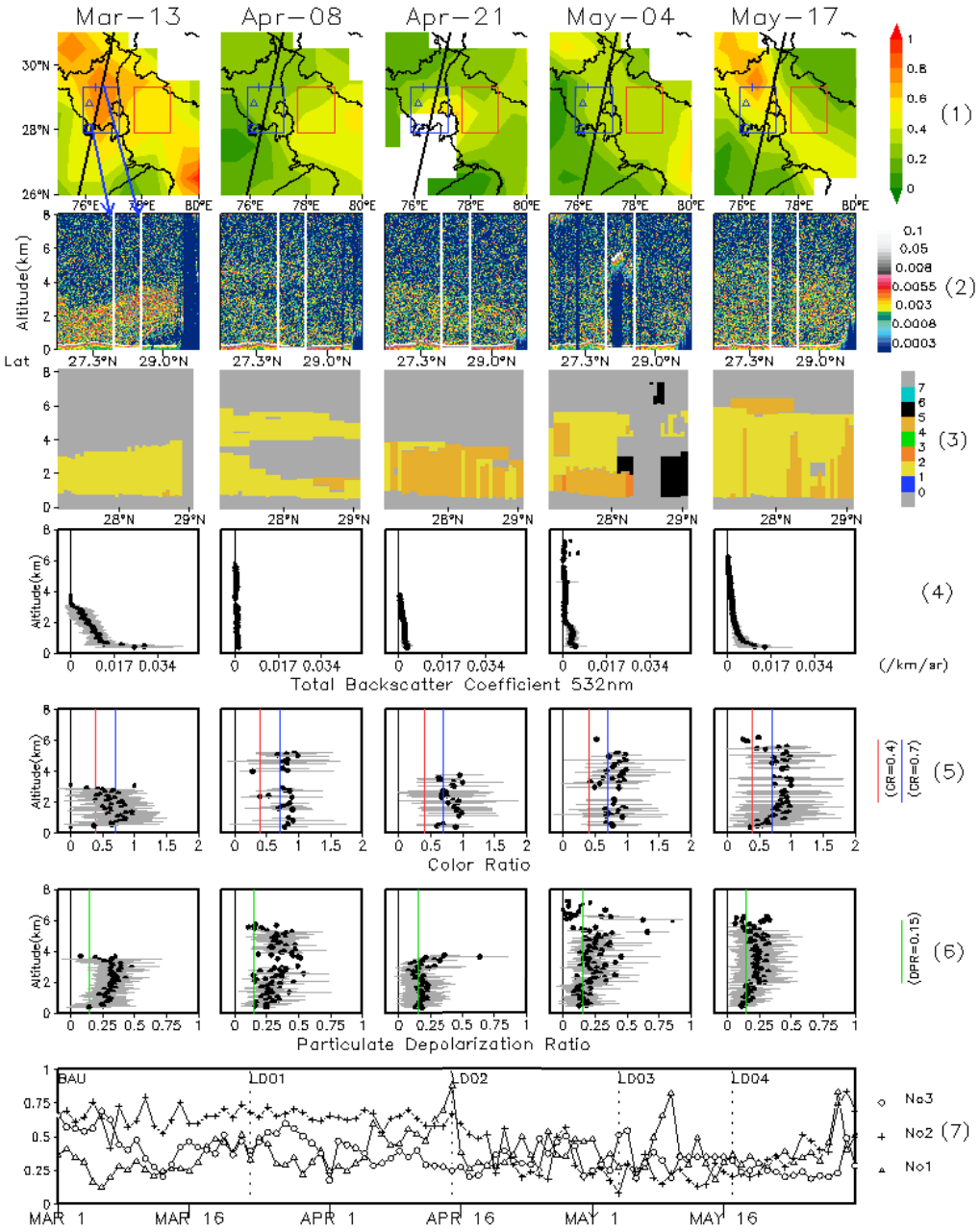

Figure 8. (1) Spatial distribution of AOD provided by MODIS, and vertical profiles from CALIPSO focusing on the Delhi-West subregion: (2) Attenuate Total Backscatter at 532 nm; (3) Aerosol types including 0-N/A, 1-clean marine, 2-dust, 3-polluted continental/smoke, 4-clean continental, 5-polluted dust, 6-elevated smoke, 7-dusty marine; Mean (black circle) and standard deviation (grey bar) of (4) Total Backscatter Coefficient at 532nm; (5) Color Ratio; and (6) Particulate Depolarization Ratio. The last row displays PM2.5/PM10 concentration ratios at Stations 1–3. The MODIS and CALIPSO data were obtained for the Delhi-West subregion for the five dates in 2020: March 13 (BAU), April 8 (Phase 1), April 21 (Phase 2), May 4 (Phase 3), and May 17 (Phase 3)

Figure 9 is similar to Fig. 8 but focuses on the Delhi-East subregion for the dates when CALIPSO had footprints over the region: March 18 (BAU), March 31 (Phase 1), April 13 (Phase 1), April 26 (Phase 2), and May 9 (Phase 3).

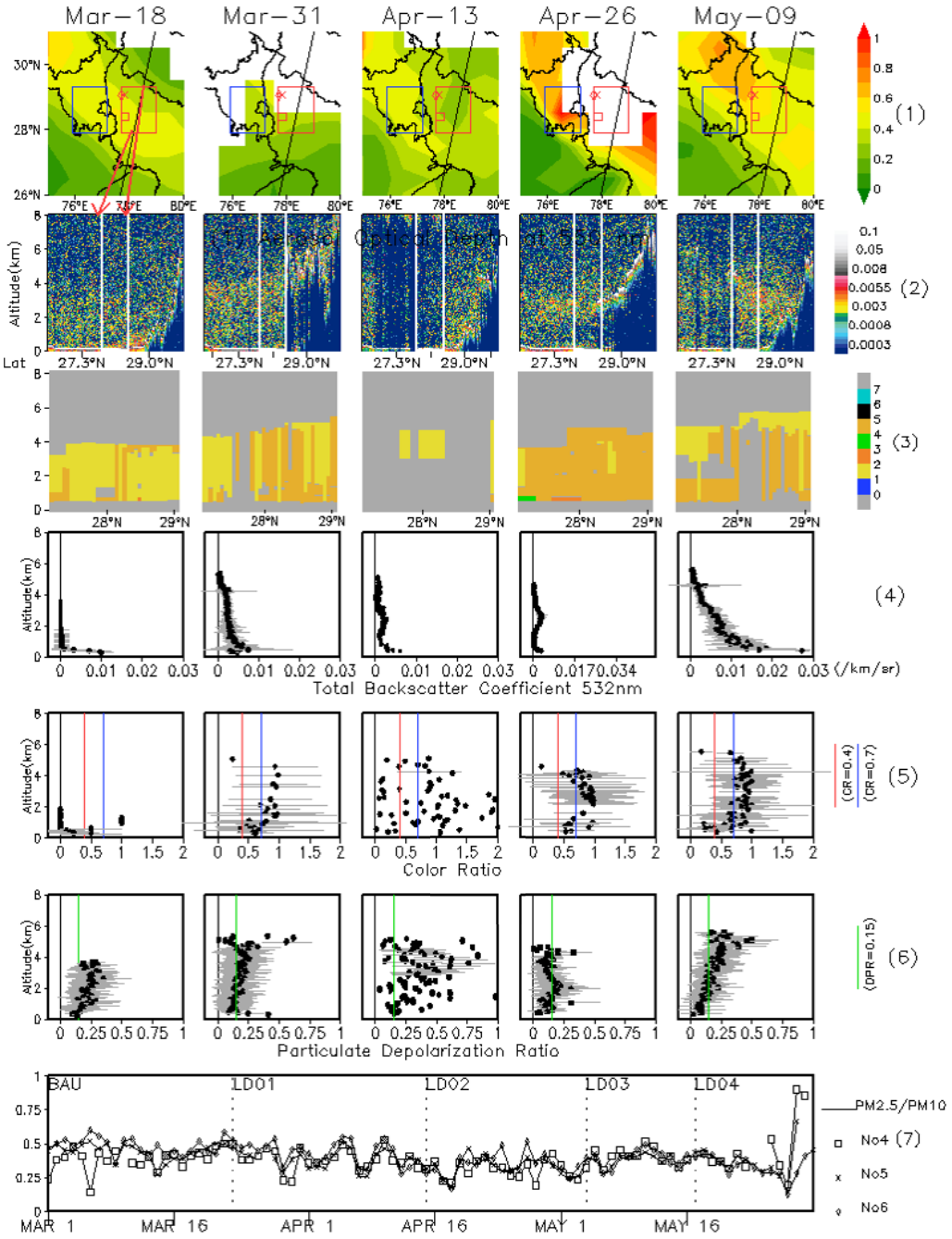

Figure 9. Similar to Fig. 8, but focusing on the Delhi-East subregion. The last row displays PM2.5/PM10 ratios at Stations 4–6. The MODIS and CALIPSO data were obtained for the five dates in 2020: March 18 (BAU), March 31 (Phase 1), April 13 (Phase 1), April 26 (Phase 2), and May 9 (Phase 3)

On March 18 (BAU), the AOD provided by MODIS was about 0.3–0.5. The CALIPSO profiles indicate an aerosol layer up to 3.5 km, as seen from the ATB Level 1 data. The aerosol types were categorized as dust and polluted dust. The vertical structure of the total backscatter coefficient (~0.01 $km^{-1}sr^{-1}$) shows slight differences across different altitudes. CR values are small at high altitudes, and the wide range of PDR values indicates fine particles with various shapes. At low altitudes, the low CR values combined with relatively small PDR values (< 0.25) indicate the dominance of fine mode and spherical particles. The PM2.5/PM10 ratios obtained from the monitoring stations are pretty stable, around 0.43, indicating a fair contribution from both natural and anthropogenic sources.

On March 31 (Phase 1), MODIS detected AOD values ranging from 0.2 to 0.4 over part of the Delhi-East subregion. The CALIPSO profiles show the presence of aerosols extending up to an altitude of 6 km (2nd, 3rd, and 4th rows in Fig. 9). Interestingly, there is almost no reduction in aerosols compared to March 13, with an increase observed at some altitudes (4th row in Fig. 9). This result may be explained by the effect of the non-local sources or the increase in household cooking emissions due to this region's high population. There are two main types of aerosols: polluted dust in the bottom layer and a mix of polluted dust and dust at the top of the aerosol layer (3rd row in Fig. 9). The CR and PDR values indicate two distinct aerosol layers: spherical and moderate size mode below 2 km and a mix of non-spherical and spherical coarse aerosols above 2 km (5th and 6th rows in Fig. 9). The PM2.5/PM10 ratios at the three monitoring stations are approximately 0.45.

On April 13 (late Phase 1), the AOD values provided by MODIS ranged from 0.2 to 0.4. The CALIPSO profiles show the existence of clouds and aerosols (2nd row in Fig. 9). There are two types of aerosols: dust above 1 km and polluted dust below 1 km. Like March 31, the total backscatter coefficient indicates no reduction in aerosols at all altitudes but rather a slight increase. The wide-ranged CR and high PDR values indicate various-sized and non-spherical particles. The PM2.5/PM10 ratios at the three monitoring stations are approximately 0.38, suggesting the relative dominance of coarse-mode dust particles over the stations. It is important to note that during this time, a mild dust storm carrying dust particles from the Thar Desert in Rajasthan and Gulf countries hit the Delhi region (CPCB, 2020), which contributed to the increase in aerosols at high altitudes and the decrease in the PM2.5/PM10 ratios in the region.

On April 26 (Phase 2), MODIS could not provide AOD information over the region. The CALIPSO profiles show a thick aerosol layer up to 4.5 km. On that day, polluted dust is dominant over dust at different altitudes. Notably, there was a mix of clean continental air, polluted dust, and polluted continental air/smoke below 1 km. The total backscatter coefficient indicates a substantial increase in aerosols at high altitudes, from 1 to 3 km. Like March 31 and April 13, the CR and PDR values indicate two distinct aerosol layers: spherical and moderate-mode aerosols below 2 km and spherical and coarse-sized aerosols above 2 km. The PM2.5/PM10 ratios at the three monitoring stations are approximately 0.3, indicating a small contribution from anthropogenic sources. Hence, the increase in aerosols at high altitudes can be attributed to non-local sources.

On May 9 (Phase 3), the AOD values provided by MODIS ranged from 0.4 to 0.6, showing a slight increase compared to March 18. The CALIPSO profiles indicate the vertical development of aerosols up to 6 km. At the top of the layer, dust covers about 1–2 km, and below that, polluted dust extends

from 1 to 5 km. Below 1 km, polluted continent/smoke appears around 28.7°N. The vertical total backscatter profile indicates a more substantial aerosol increase at different altitudes compared to March 18. A pair of relatively high CR (>0.8) and low PDR (mostly >0.2) values indicate the presence of coarse and spherical aerosols above 1 km. Below 1 km, CR exhibited both relatively high (>0.7), 0.4–0.7, and low values (<0.4), while PDR remained low (<0.15), indicating a mix of fine and coarse spherical aerosols near the surface. The PM2.5/PM10 ratios at the three monitoring stations are about 0.4, suggesting small contributions from local anthropogenic sources, which can be explained by the fact that the three stations were in the red zone on May 9. Therefore, the increase in aerosols at higher altitudes can be attributed to non-local sources.

3.3. Changes in surface aerosols

It is crucial to quantify aerosol values close to the surface to understand the severity of pollution and its potential negative impact on human health and other societal activities. However, aerosol information below approximately 300 m is often missing in CALIPSO data. Therefore, we analyze variations in PM2.5 and PM10 for the surface layer, which are often classified as fine aerosols due to their small size and ability to remain suspended in the air. These PM values were observed at the six monitoring stations, with Stations 1–3 located in Delhi-West and Stations 4–6 in Delhi-East (Fig. 10). The advantage of using these monitoring stations is the continuity of the data, which provides much better temporal coverage than satellite information. In Figs. 8 and 9, we already discussed the PM2.5/PM10 ratios, which can indicate whether pollutants were primarily emitted from anthropogenic or natural sources. In Fig. 10, we focus on the variations of PM2.5 and PM10 concentrations rather than their ratios.

Before the lockdown, Delhi-East exhibited higher PM concentrations and more considerable variations than Delhi-West. The lockdown imposed on March 23 induced a remarkable reduction in PM concentration in both Delhi-West and Delhi-East, with daily PM2.5 (PM10) values dropping by up to 10–15 (25–45) $\mu g.m^{-3}$ in Delhi-West and 10–20 (30) $\mu g.m^{-3}$ in Delhi-East. These reductions were slightly lower than those reported for Delhi-Central (Dhaka et al., 2020; Sathe et al., 2021).

The decrease in PM2.5 concentrations during Phase 1 resulted from the combined effect of the lockdown and heavy rainfall in northern India during the first week of the lockdown. PM levels in both subregions remained low for about a week after that. These PM concentration values and their variability can be considered as the natural characteristics of PMs without anthropogenic emissions in the regions, as Dhaka et al. (2020) suggested. From the second week of April 2020, increases in PM levels were observed, except at Station 1. It is noted that PM10 levels at Station 1 remain pretty stable during the lockdown phases with lower values compared to the BAU period. Notably, PM2.5 levels are generally higher in Delhi-East compared to Delhi-West. This difference is exciting given Delhi-East's higher population density, suggesting the significant role of anthropogenic activities in PM2.5 emission, even during the lockdown period: as people spent more time indoors, there was an increase in household coal combustion, likely due to cooking activities. Regarding PM10, there was a significant rise at almost all stations between the 13^{th} and 16^{th} of April 2020 due to the impact of a minor dust storm transporting particulate matter from the Thar Desert in Rajasthan and Gulf countries to the Delhi-NCR region (CPCB, 2020).

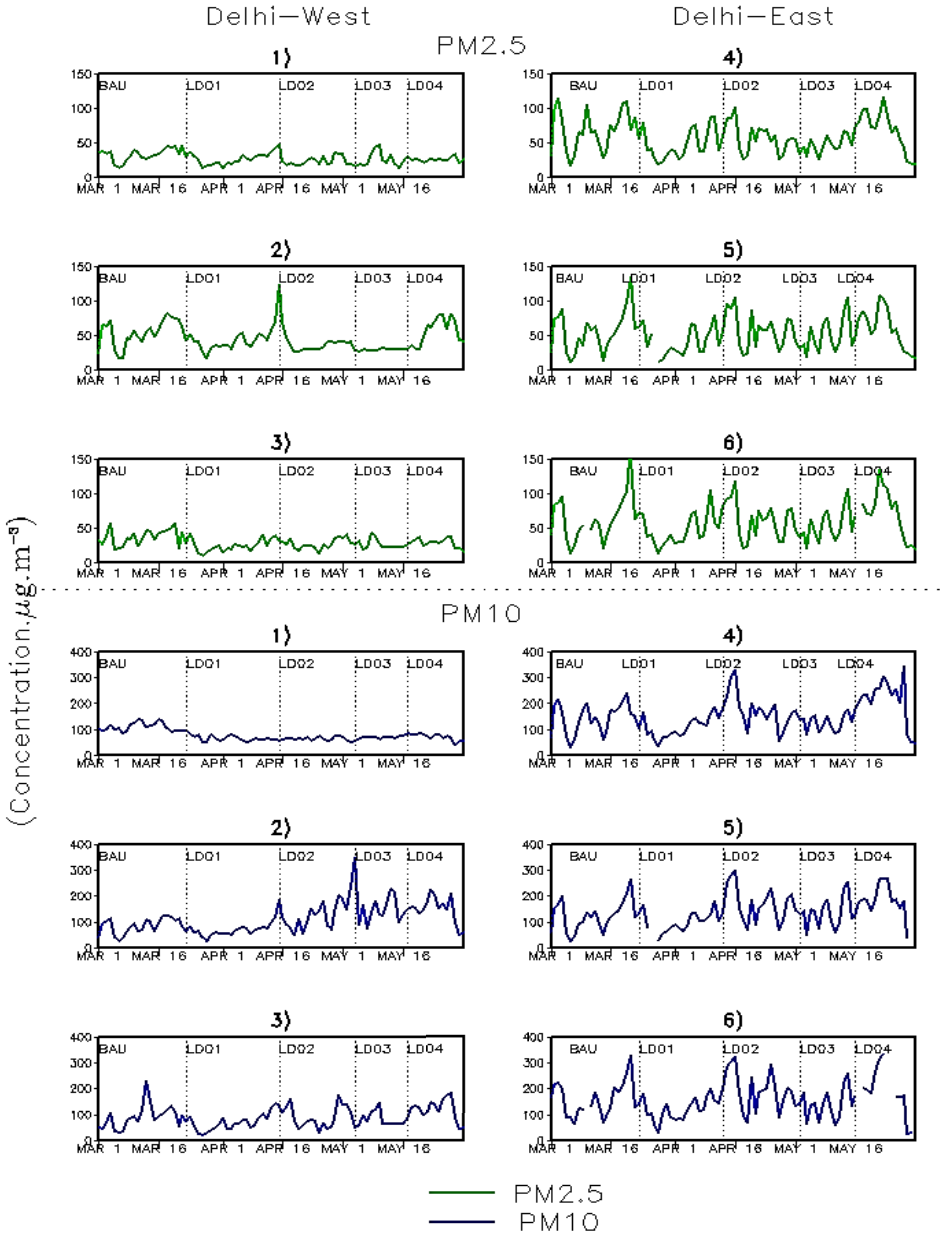

Figure 10. Temporal evolution of daily mean PM2.5 and PM10 concentration (unit is μg.m^{-3}) at 6 stations before and during the lockdown period

We further investigate the diurnal variability of PM to understand the link between the footprint of human activities and air pollution. Figure 11 illustrates the changes in PM diurnal variations under BAU and during different phases of the lockdown. It should be noted that meteorological conditions, daytime and nighttime chemistry, and local emissions generally influence PM diurnal variations. The closures of non-essential services and offices and restrictions on the movement of people result in a reduction of anthropogenic emissions, leading to alterations in the levels of PM at various

times during the day. Singh et al. (2020b) demonstrated significant changes in fuel consumption during the lockdown period across various sectors: a reduction of 50–60% in transport, 90% in aviation, 40% in industry, and 70% in construction activities, along with an increase of approximately 12% in household fuel consumption. The minimum PM concentration was noted during the late afternoon period, specifically between 15:00 and 16:00, across all monitoring stations (Fig. 11). For the Delhi-East stations, two distinct peaks were observed during the day: morning and evening.

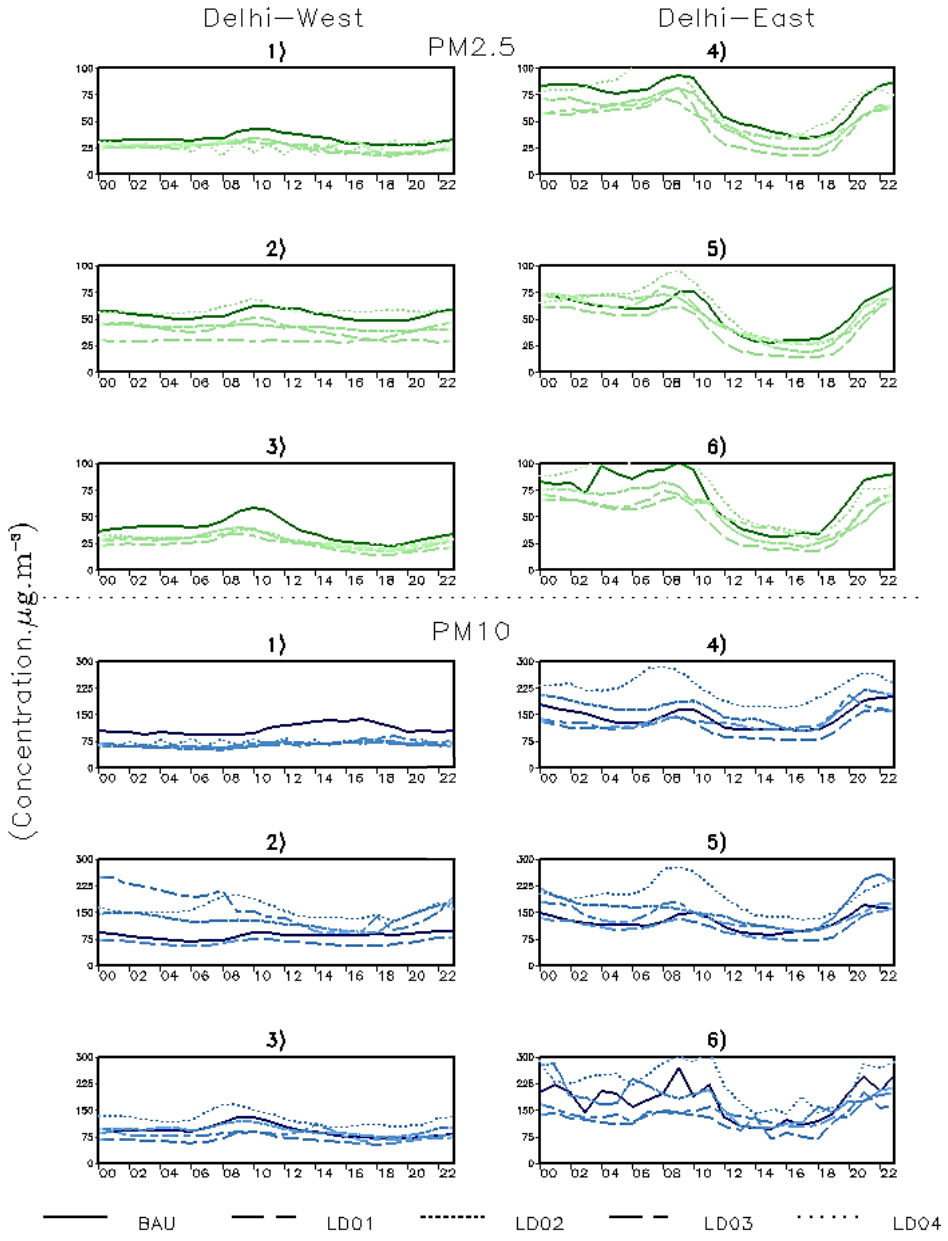

Figure 11. Diurnal variations of PM2.5 and PM10 (units is μg.m^{-3}) at 6 stations before and during the lockdown period

Conversely, Delhi-West experienced a single peak in the morning hours. The morning peak, observed between 08:00 and 10:00, can be attributed to the combined effects of fumigation and traffic-related emissions.

On the other hand, the rise in pollution levels during the evening and night is linked to traffic activities and household emissions (Yadav et al., 2017; Ravindra et al., 2019; Kaur-Sidhu et al., 2020; Singh et al., 2020a) and lower dispersion due to reduced planetary boundary level height (Schnell et al., 2018). The secondary peak detected at the Delhi-East stations during late night hours from 20:00 to 23:00 local time may be partially attributed to evening traffic congestion, predominantly caused by heavy diesel vehicles. This phenomenon is exacerbated by the shallow nocturnal boundary layer conditions and reduced wind speeds characteristic of nighttime (Srivastava et al., 2021).

An apparent decrease in PM2.5 levels at the monitoring station indicates reduced emissions during the lockdown phases. PMs were at notably lower levels during Phase 1 than subsequent phases. Singh et al. (2021) suggested that the more significant decrease in PM10 levels compared to PM2.5 levels during the initial phase of the lockdown can be attributed to the decrease in construction activities and the decrease in dust resuspension due to reduced vehicular movement. Regarding PM10, it is worth noting that the presence of dust storms, combined with the partial easing of lockdown measures during LD02–4, increases PM10 concentration during these phases (Fig. 11).

4. Conclusions

Our study utilized three different data sources, including MODIS, CALIPSO, and station data, to assess aerosol changes, focusing on two specific regions: Delhi-West and Delhi-East.

We observed a remarkable decrease in AOD across a large area of Delhi-NCR during the lockdown phases. Particularly noteworthy is Phase 1, which exhibited the largest significant decrease compared to the other phases. The higher AOD in Delhi-East during the early lockdown phases, compared to Delhi-West, is attributed to its higher population density. Conversely, the intensification of AOD in Delhi-West from Phase 3 onwards can be attributed to natural sources such as dust storms. Using CALIOP data, the contribution of aerosols across different vertical layers during the lockdown phases was assessed for the first time. Generally, aerosols are concentrated in the lower layer, with approximately 40% of the total AOD attributed to aerosols below 1 km. The surface observations revealed that PM2.5 levels in Delhi-East are generally higher compared to Delhi-West due to its higher population density. This disparity underscores the significant impact of anthropogenic activities on PM2.5 emissions, even during the lockdown period. Additionally, there was a notable increase in PM10 levels on some lockdown dates, attributed to minor dust storms from long-range transportation.

It is worth noting that higher-resolution MODIS products may yield different results, especially when comparing MODIS and CALIOP data. In the present study, the three data sources were used complementarily to assess aerosol changes over Delhi-NCR during the lockdown period. In further research, conducting a more detailed analysis using these datasets across different regions would be of great interest. Furthermore, investigating the sensitivity of the results to the choice of datasets and exploring the association between aerosol quantities and local and distant meteorological factors should also be considered.

Acknowledgments

The authors would like to thank Professor Hayashida Sachiko, Dr. Prakhar Misra, and

the DELHIS Mission Team under WG2 of the Aakash project for their support of the study. H. Nguyen-Thuy is grateful to the Ministry of Education, Culture, Science, and Technology (MEXT) for the scholarship support to pursue higher education at Nara Women's University. We acknowledge the Central Pollution Control Board (CPCB) the NASA and CNES teams for providing us access to their data products.

References

Babu S.S., Manoj M.R., Moorthy K.K., Gogoi M.M., Nair V.S., Kompalli S.K., Satheesh S.K., Niranjan K., Ramagopal K., Bhuyan P.K., Singh D., 2013. Trends in aerosol optical depth over Indian region: Potential causes and impact indicators. Journal of Geophysical Research: Atmospheres, 11, 794.

Balk D., Montgomery M.R., Engin H., Lin N., Major E., Jones B., 2019. Urbanization in India: Population and Urban Classification Grids for 2011. Data (MDPI), 4, 35.

Bamola S., Goswami G., Dewan S., Goyal I., Agarwal M., Dhir A., Lakhani A., 2024. Characterising temporal variability of PM2.5/PM10 ratio and its correlation with meteorological variables at a sub-urban site in the Taj City. Urban Climate, 53, 101763.

Brasseur G., Orlando J.J., Tyndall G.S. (Eds.), 1999. Atmospheric chemistry and global change. New York: Oxford University Press.

Chandra S., Dwivedi A.K., Kumar M., 2014. Characterization of the atmospheric boundary layer from radiosonde observations along eastern end of monsoon trough of India. Journal of Earth System Science, 123, 1233–1240.

Central Pollution Control Board (CPCB), Delhi, 2020. Impact of lockdown (March 25 to April 15) on air quality. Ministry of Environment, Forest and Climate Change, Govt of India.

David L.M., et al., 2018. Aerosol Optical Depth Over India. Journal of Geophysical Research: Atmospheres, 123, 3688–3703.

Dey S., Tripathi S.N., Singh R.P., Holben B.N., 2004. Influence of dust storms on the aerosol optical properties over the Indo-Gangetic basin. Journal of Geophysical Research: Atmospheres, 109, D20211.

Dey S., Tripathi S.N., Mishra S.K., 2008. Probable mixing state of aerosols in the Indo-Gangetic Basin, northern India. Geophysical Research Letter, 35, L03808.

Dhaka S.K., Chetna Kumar V., Panwar V., Dimri A.P., Singh N., Patra P.K., Matsumi Y., Takigawa M., Nakayama T., Yamaji K., Kajino M., Misra P., Hayashida S., 2020. PM2.5 diminution and haze events over Delhi during the COVID-19 lockdown period: an interplay between the baseline pollution and meteorology. Scientific Reports, 10, 13442.

Dimitrova A., Bora J.K., 2020. Monsoon weather and early childhood health in India. PLoS ONE, 15(4), e0231479.

Esri India Technologies Private Limited., 2023. India: State boundary 2021 and India: District boundary 2021. https://policymaps.esri.in/datasets (last accessed March 21, 2024).

Eeftens M., et al., 2012. Spatial variation of PM2.5, PM10, PM2.5 absorbance and PM coarse concentrations between and within 20 European study areas and the relationship with NO_2 - Results of the ESCAPE project. Atmospheric Environment, 62, 303–317.

Fan H., Zhao C., Yang Y., Yang X., 2021. Spatio-Temporal Variations of the PM2.5/PM10 Ratios and Its Application to Air Pollution Type Classification in China. Frontiers in Environmental Science, 9, 692440.

Fujimori S., Hasegawa T., Ito A., Takahashi K., Masui T., 2018. Gridded emissions and land-use data for 2005–2100 under diverse socioeconomic and climate mitigation scenarios. Scientific Data, 5, 180210.

Gautam R., Hsu N.C., Lau K.M., Kafatos M., 2009. Aerosol and rainfall variability over the Indian monsoon region: distributions, trends and coupling. Annales Geophysicae, 9, 3691–3703.

Gautam R., Hsu N.C., Lau K.M., 2010. Premonsoon aerosol characterization and radiative effects over the Indo-Gangetic Plains: Implications for regional climate warming. Journal of Geophysical Research: Atmospheres, 115, D17208.

Gouda K.C., Gogeri I., ThippaReddy A.S., 2022. Assessment of Aerosol Optical Depth over Indian Subcontinent during COVID-19 lockdown (March-May 2020). Environmental Monitoring and Assessment, 194, 195.

Guttikunda S.K., Mohan D., 2014. Re-fueling road transport for better air quality in India. Energy Policy, 68, 556–561.

Habib A., Chen B., Khalid B., Tan S., Che H., Mahmood T., Butt M., 2019. Estimation and inter-comparison of dust aerosols based on MODIS, MISR and AERONET retrievals over Asian desert regions. Journal of Environmental Sciences, 76, 154–166.

Hamed K.H., 2008. Trend detection in hydrologic data: The Mann–Kendall trend test under the scaling hypothesis. Journal of Hydrology, 349, 350–363.

Hayes C. R., Coakley Jr. J. A.,Tahnk W. R., 2010. Relationships among properties of marine stratocumulus derived from collocated CALIPSO and MODIS observations. Journal of Geophysical Research: Atmospheres, 115 (D4).

Jethva H., Chand D., Torres O., Gupta P., Lyapustin A., Patadia F., 2018. Agricultural burning and air quality over northern India: a synergistic analysis using NASA's A-train satellite data and ground measurements. Aerosol and Air Quality Research, 18, 1756–1773.

Kanawade V.P., Srivastava A.K., Ram K., Asmi E., Vakkari V., Soni V.K., Varaprasad V., Sarangi C., 2020. What caused severe air pollution episode of November 2016 in New Delhi?. Atmospheric Environment, 222, 117125.

Kaur-Sidhu M., Ravindra K., Mor S., John S., 2020. Emission factors and global warming potential of various solid biomass fuel-cook stove combinations. Atmospheric Pollution Research, 11(2), 252–260.

Kendall M.G., 1938. A New Measure of Rank Correlation. Biometrika, 30(1/2), 81–93.

Khodeir M., Shamy M., Alghamdi M., Zhong M., Sun H., Costa M., Chen L.C., Maciejcczyk P.M., 2012. Source apportionment and elemental composition of PM2.5 and PM10 in Jeddah City, Saudi Arabia. Atmospheric Pollution Research, 3, 331–340.

Kim M.H., Omar A.H., Tackett J.L., Vaughan M.A., Winker D.M., Trepte C.R., Hu Y., Liu Z., Poole L.R., Pitts M.C., Kar J., Magill B.E., 2018. The CALIPSO version 4 automated aerosol classification and lidar ratio selection algorithm. Atmospheric Measurement Technique, 11, 6107–6135.

Kliengchuay W., Mingkhwan R., Kiangkoo N., Kongpran J., Aung H.W., Tantrakarnapa K., 2024. Analyzing temperature, humidity, and precipitation trends in six regions of Thailand using innovative trend analysis. Scientific Reports, 14, 7800.

Kumar M., Parmar K.S., Kumar D.B., Mhawish A., Broday D.M., Mall R.K, Banerjee T., 2018. Long-term aerosol climatology over Indo-Gangetic Plain: trend, prediction and potential source fields. Atmospheric Environment, 180, 37–50.

Lau K.M., Kim K.M., 2006. Observational relationship betweenAerosol and Asian monsoon rainfall, and circulation. Geophysical Research Letters, 33, L21810.

Lau K.M., Kim M.K., Kim K.M., 2006. Asian summer monsoon anomalies induced by aerosol direct forcing: the role of the Tibetan Plateau. Climate Dynamics, 26, 855–864.

Lelieveld J., Evans J.S., Fnais M., Giannadaki D., Pozzer A., 2015. The contribution of outdoor air pollution sources to premature mortality on a global scale. Nature, 525(7569), 367-371.

Levy R.C., Mattoo S., Munchak L.A., Remer L.A., Sayer A.M., Patadia F., Hsu N.C., 2013. The Collection 6 MODIS aerosol products over land and ocean. Atmospheric Measurement Techniques, 6, 2898–3034.

Levy R.C., Mattoo S., Sawyer V., Shi Y., Colarco P.R., Lyapustin A.I., Wang Y., Remer L.A., 2018. Exploring systematic offsets between aerosol products from the two MODIS sensors. Atmospheric Measurement Techniques, 11, 4073–4092.

Liou K.N., 2002. An Introduction to Atmospheric Radiation. Elsevier, 84, 1–583.

Liu T., Marlier M.E., DeFries R.S., Westervelt D.M., Xia K.R., Fiore A.M., Mickley L.J., Cusworth D.H., Milly G., 2018. Seasonal impact of regional outdoor biomass burning on air pollution in three Indian

cities: Delhi, Bengaluru, and Pune. Atmospheric Environment, 172(83–92), 1352–2310.

Liu Z., Omar A., Vaughan M., Hair J., Kittaka, C., Hu Y., Powell K., Trepte C., Winker D., Hostetler C., Ferrare R., Pierce R., 2008. CALIPSO lidar observations of the optical properties of Saharan dust: A case study of long-range transport. Journal of Geophysical Research Atmospheres, 113 (D7).

Liu Z., Vaughan M., Winker D., Kittaka C., Getwewich B., Kuehn R., Omar A., Powell K., Trepte C., Hostetler C., 2009. The CALIPSO lidar cloud and aerosol discrimination: Version 2 algorithm and initial assessment of performance. Journal of Atmospheric and Oceanic Technology, 26, 1198–1213.

Mahato S., Pal S., Ghosh K.G., 2020. Effect of lockdown amid COVID-19 pandemic on air quality of the megacity Delhi, India. Science of The Total Environment, 730, 139086.

Mann H.B., 1945. Nonparametric Tests Against Trend. Econometrica, 13(3), 245–259.

Mehta M., Khushboo R., Raj R., Singh N., 2021. Spaceborne observations of aerosol vertical distribution over Indian mainland (2009–2018). Atmospheric Environment, 244, 117902.

Ministry of Home Affairs, 2020. Guidelines on the measure to be taken by Ministers/Departments of Government of India, State/Union Territory Governments and State/Union Territory Authorities for Containment of COVID-19 epidemic in the country.

Mishra A.K., Shibata T., 2012. Climatological aspects of seasonal variation of aerosol vertical distribution over central Indo-Gangetic belt (IGB) inferred by space-borne lidar CALIOP. Atmospheric Environment, 46, 365–375.

Misra P., Takigawa M., Khatri P., Dhaka S.K., Dimri A.P., Yamaji K., Kajino M., Takeuchi W., Imasu R., Nitta K., Patra P.K., Hayashida S., 2021. Nitrogen oxides concentration and emission change detection during COVID-19 restrictions in North India. Scientific Reports, 11, 9800.

Nakoudi K., Giannakaki, E., Dandou, A., Tombrou, M., Komppula, M., 2019. Planetary boundary layer height by means of lidar and numerical simulations over New Delhi, India. Atmospheric Measurement Techniques, 12(5), 2595–2610.

Nigam S., Bollasina M., 2010. "Elevated heat pump" hypothesis for the aerosol-monsoon hydroclimate link: "Grounded" in observations?. Journal of Geophysical Research, 115, D16201.

Nirwan N., Siddiqui A., Kannemadugu H.B.S., Chauhan Pr., Singh R.P., 2024. Determining hotspots of gaseous criteria air pollutants in Delhi airshed and its association with stubble burning. Scientific Reports, 14, 986.

Pandey S.K., Vinoj V., 2021. Surprising Changes in Aerosol Loading over India amid COVID-19 Lockdown. Aerosol and Air Quality Research, 21(3), 200466.

Pandithurai G., Dipu S., Dani K.K., Tiwari S., Bisht D.S., Devara P.C.S., Pinker R.T., 2008. Aerosol radiative forcing during dust events over New Delhi, India. Journal of Geophysical Research: Atmospheres, 113, D13209.

Platnick S., et al., 2015. MODIS Atmosphere L3 Daily Product. NASA MODIS Adaptive Processing System, Goddard Space Flight Center, USA.

Prijith S.S., Srinivasulu J., Sesha Sai M.V.R., 2021. Dominance of natural aerosols over India in pre-monsoon: inferences from the lockdown effects. Current Science, 120(2), 25.

Rani S., Kumar R., 2022. Spatial distribution of aerosol optical depth over India during COVID-19 lockdown phase-1. Spatial Information Research, 30, 417–426.

Ravindra K., Singh T., Mor S., Singh V., Mandal T.K., Bhatti M.S., Gahlawat S.K., Dhankhar R., Beig G., 2019. Real-time monitoring of air pollutants in seven cities of North India during crop residue burning and their relationship with meteorology and transboundary movement of air. Science of The Total Environment, 690, 717–729.

Salerno F., Guyennon N., Yang K., Shaw T.E., Lin C., Colombo N., Romano E., Gruber S., Bolch T., Alessandri A., Cristofanelli P., Putero D., Diolaiuti G., Tartari G., Verza G., Thakuri S., Balsamo G., Miles E.S., Pellicciotti F., 2023. Local cooling and drying induced by Himalayan glaciers under global warming. Nature Geoscience, 16(12), 1120–1127.

Sathe Y., Gupta P., Bawase M., Lamsal L., Patadia F., Thipse S., 2021. Surface and satellite observations of air pollution in India during COVID-19 lockdown: Implication to air quality. Sustainable Cities and Society, 66, 102688.

Sathyanadh A., Prabhakaran T., Patil C., Karipot A., 2017. Planetary boundary layer height over the Indian subcontinent: Variability and controls with respect to monsoon. Atmospheric Research, 195, 44–61.

Sharma V., Ghosh S., Shahnawaz S., Rai P.K., Singh S., 2022. Covid-19 lockdown effect on aerosol optical depth in Delhi National Capital Region, India. Forum Geografic, XXI, 146–157.

Sayer A.M., Hsu N.C., Bettenhausen C., Jeong M.J., 2013. Validation and uncertainty estimates for MODIS Collection 6 "Deep Blue" aerosol data. Journal of Geophysical Research: Atmospheres, 118(14), 7864–7872.

Sayer A.M., Munchak L.A., Hsu N.C., Levy R.C., Bettenhausen C., Jeong M.J., 2014. MODIS Collection 6 aerosol products: Comparison between Aqua's e-Deep Blue, Dark Target, and "merged" data sets, and usage recommendations. Journal of Geophysical Research: Atmospheres, 119, 13965–13989.

Sharma R., Joshi P.K., 2016. Mapping environmental impacts of rapid urbanization in the national capital region of India using remote sensing inputs. Urban Climate, 15, 70–82.

Shiraiwa M., Ammann M., Koop T., Pöschl U., 2011. Gas uptake and chemical aging of semisolid organic aerosol particles. Proceedings of the National Academy of Sciences, 108(27), 11003–11008.

Singh S., Nath S., Kohli R., Singh R., 2005. Aerosol over Delhi during pre-monsoon months: characteristics and effects on surface radiation forcing. Geophysical Research Letters, 32, L13808.

Singh V., Biswal A., Kesarkar A.P., Mor S., Ravindra K., 2020a. High resolution vehicular PM10 emissions over megacity Delhi: relative contributions of exhaust and non-exhaust sources. Science of The Total Environment, 699, 134273.

Singh V., Singh S., Biswal A., Kesarkar A.P., Mor S., Ravindra K., 2020b. Diurnal and temporal changes in air pollution during COVID-19 strict lockdown over different regions of India. Environmental Pollution, 266, 115368.

Singh V., Singh S., Biswal A., 2021. Exceedances and trends of particulate matter (PM2.5) in five Indian megacities. Science of Total Environment, 750, 141461.

Schnell J.L., Naik V., Horowitz L.W., Paulot F., Mao J., Ginoux P., Zhao M., Ram K., 2018. Exploring the relationship between surface PM2.5 and meteorology in Northern India. Atmospheric Chemistry and Physics, 18, 10157–10175.

Soni P., 2021. Effects of COVID-19 lockdown phases in India: an atmospheric perspective. Environment, Development and Sustainability, 23(8), 12044–12055.

Srivastava A.K., Bhoyar P.D., Kanawade V.P., Devara P.C.S., Thomas A., Soni V.K., 2021. Improved air quality during COVID-19 at an urban megacity over the Indo-Gangetic-Basin: From stringent to relaxed lockdown phases. Urban Climate, 36, 100791.

Sugimoto N., Matsui I., Shimizu A., Uno I., Asai K., Endoh T., Nakajima T., 2002. Observation of dust and anthropogenic aerosol plumes in the Northwest Pacific with a two-wavelength polarization lidar on board the research vessel Mirai. Geophysical Research Letters, 29(19), 1901.

Sugimoto N., Shimizu A., Matsui I., Nishikawa M., 2016. A method for estimating the fraction of mineral dust in particulate matter using PM2.5-to-PM10 ratios. Particuology, 28, 114–120.

Tariq S., Qayyum F., Ul-Haq Z., Mehmood U., 2022. Long-term spatiotemporal trends in aerosol optical depth and its relationship with enhanced vegetation index and meteorological parameters over South Asia. Environmental Science and Pollution Research, 29(20), 30638–30655.

Tripathi S.N., Pattnaik A., Dey S., 2007. Aerosol indirect effect over Indo- Gangetic plain. Atmospheric Environment, 41, 7037–7047.

Venkat-Ratnam M., Prasad P., Akhil Raj S.T., Hoteit I., 2021. Effect of Lockdown due to COVID-19 on the Aerosol and Trace Gases Spatial Distribution over India and Adjoining Regions. Aerosol and Air Quality Research, 21(2), 200397.

Vu-Thanh H., Ngo-Duc T., Phan-Van T., 2014. Evolution of meteorological drought characteristics in Vietnam during the 1961-2007 period. Theoretical and Applied Climatology, 118(3), 367–375.

Wandinger U., Anja H., Ina M., Gelsomina P., Lucia M., Fabio M., 2011. Aerosols and Clouds: Long-term Database from Spaceborne Lidar Measurements. Leibniz Institute for Tropospheric Res https://www.tropos.de/fileadmin/user_upload/Institut/Abteilungen/Fernerkundung/Daten_PDF/Wandinger-ESA_2011.pdf (last accessed 1 August 2024).

Wilcoxon F., 1945. Individual comparisons by ranking methods. Biometrics Bulletin, 1(6), 80–83.

Winker D.M., Vaughan M.A., Omar A., Hu Y., Powell K.A., Liu Z., Hunt W.H., Young S.A., 2009. Overview of the CALIPSO Mission and CALIOP Data Processing Algorithms. Journal of Atmospheric and Oceanic Technology, 26, 2310–2323.

World Health Organization (WHO), 2016. Ambient air pollution: A global assessment of exposure and burden of disease. WHO Publication. https://www.who.int/publications/i/item/9789241511353.

World Health Organization (WHO), 2021. WHO global air quality guidelines: particulate matter (PM2.5 and PM10), ozone, nitrogen dioxide, sulfur dioxide and carbon monoxide. WHO Publication. https://www.who.int/publications/i/item/9789240034228.

Yadav R., Sahu L.K., Beig G., Tripathi N., Jaaffrey S.N.A., 2017. Ambient particulate matter and carbon monoxide at an urban site of India: influence of anthropogenic emissions and dust storms. Environmental Pollution, 225, 291–303.